

## Nonstoichiometry and the Electrical Activity of Grain Boundaries in SrTiO<sub>3</sub>

Miyoung Kim,<sup>1,2</sup> Gerd Duscher,<sup>1,3</sup> Nigel D. Browning,<sup>2</sup> Karl Sohlberg,<sup>1</sup>  
Socrates T. Pantelides,<sup>1,3</sup> and Stephen J. Pennycook<sup>1,3</sup>

<sup>1</sup>*Solid State Division, Oak Ridge National Laboratory, Oak Ridge, Tennessee 37831-6030*

<sup>2</sup>*Department of Physics, University of Illinois at Chicago, Chicago, Illinois 60612*

<sup>3</sup>*Department of Physics and Astronomy, Vanderbilt University, Nashville, Tennessee 37235*

(Received 1 June 2000)

A combination of experiments and first-principles calculations is used to show that grain boundaries in SrTiO<sub>3</sub> are intrinsically nonstoichiometric. Total-energy calculations reveal that the introduction of nonstoichiometry into the grain boundaries is energetically favorable and results in structures that are consistent with atomic-resolution *Z*-contrast micrographs. Electron energy-loss spectra provide direct evidence of nonstoichiometry. These results and calculations for nonstoichiometric grain boundaries provide an explanation of the microscopic origin of the “double Schottky barriers” that dominate the electrical behavior of polycrystalline oxides.

DOI: 10.1103/PhysRevLett.86.4056

PACS numbers: 61.72.Mm, 68.37.Lp, 71.15.Nc, 82.20.Pm

The electrical activity of grain boundaries is responsible for the nonlinear *I*-*V* characteristics [1] of perovskites used in barrier-layer devices such as capacitors and varistors [2,3]. SrTiO<sub>3</sub> is a model system for perovskites as well as for oxide superconductors, for which similar models for electrical activity have been proposed [4]. Grain boundaries are also likely to profoundly affect properties such as domain wall motion in ferroelectric, magnetic, and magnetoresistive perovskites [5,6].

The macroscopic electrical properties of SrTiO<sub>3</sub> are usually explained phenomenologically in terms of double Schottky barriers that are assumed to originate from charged grain boundary planes and the compensating space charge in the corresponding depletion layers [7,8]. The net result is an electrostatic potential (band bending) that opposes the passage of free carriers through the grain boundary. However, the microscopic origin of this phenomenon has remained elusive. In pristine materials, it has long been assumed that the charge arises from intrinsic point defects that form because of lower formation energies at the boundary [9,10], but the identity of such defects has not been established. In doped materials, the charge at grain boundaries is believed to be altered by impurity segregation [10]. Both conventional and *Z*-contrast transmission electron microscopy images of SrTiO<sub>3</sub> grain boundaries have been found to be consistent with stoichiometric structures [11–13]. First-principles theoretical work on this and other similar grain boundaries (e.g., in TiO<sub>2</sub>) *assumed* stoichiometry and found that there are no localized states in the energy gap [14,15].

In this Letter, we use a combination of experimental and computational results to show that grain boundaries in SrTiO<sub>3</sub> are intrinsically *nonstoichiometric*. We first present high-spatial-resolution electron energy-loss spectra (EELS) showing that the ratio of Ti to O atoms in the grain boundary is larger than in the bulk (O deficiency or Ti excess). We then present a series of first-principles theoretical results that show that the lowest-energy grain

boundary structures are nonstoichiometric *and* consistent with atomic-resolution *Z*-contrast micrographs [11–15]. The dominant feature is a larger Ti:O ratio in the grain boundary, as found by EELS. We also report calculations of the electron density of nonstoichiometric grain boundaries and show that the so-called double Schottky barrier is better described as a *p-n-p* double junction where the grain boundary is “doped” by segregated excess Ti and O deficiency.

Dedicated scanning transmission electron microscopes (STEM) were used in this study with probe sizes close to 2.2 (VG HB501 UX) and 1.3 Å (VG HB603 U). Dark-field *Z*-contrast images in which the intensity of each atomic column is directly related to the atomic number *Z* [16] provided initial structures for total-energy calculations. Columns containing Sr and Ti are distinguished directly from the image without the need for simulations, whereas O columns are invisible. An example of a *Z*-contrast image is shown in Fig. 1. EELS data from selected atomic columns provide a sensitive probe of local

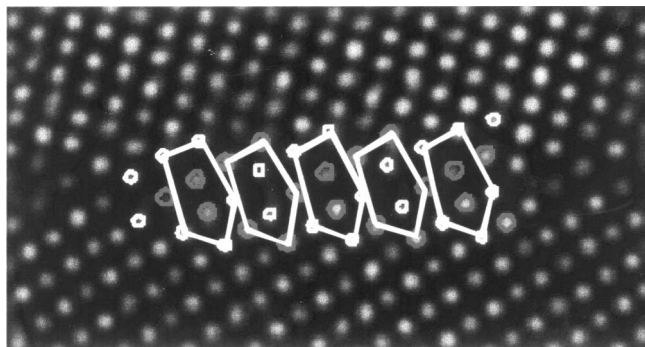


FIG. 1. A *Z*-contrast image showing dislocation core units in a SrTiO<sub>3</sub> 36° [001] symmetric tilt grain boundary. The pairs of columns within the pentagons were previously assumed to be half-occupied to avoid nonstoichiometry. In this paper, we show that they are in fact nonstoichiometric.

composition and electronic structure [17–19]. The data are shown in Fig. 2 and will be discussed below.

The calculations used the local-density approximation [20,21] for the exchange-correlation potential, ultrasoft pseudopotentials [22] with a plane wave energy cutoff of 380 eV, the Monkhorst-Pack scheme [23] for Brillouin zone  $k$ -point sampling, and the all-bands scheme [24] for electronic minimization. The  $3s$ ,  $3p$ ,  $4s$ , and  $3d$  electrons were included as valence electrons for Ti, and the  $4s$ ,  $4p$ , and  $5s$  electrons were included for Sr. In bulk  $\text{SrTiO}_3$ , the experimental value of the lattice constant is 3.905 Å while the theoretical value is 3.863 Å, in agreement with previous theoretical calculations [11,25]. For the grain-boundary calculations, supercells were set up containing two parallel boundaries to enable periodic boundary conditions. The structure was allowed to relax freely perpendicular to the boundaries except for atoms in the bulk layer between the two grain boundaries, which were fixed. Cell expansion was allowed only in the direction perpendicular to the grain boundary plane. Relaxation continued until the residual forces reached 0.05 eV/Å, and the residual energy reached  $2 \times 10^{-3}$  eV/atom. The standard supercell used in the calculations contains 100 atoms. The computations are very time consuming, but limited convergence studies were carried out. Calculations of O vacancies in a grain boundary were performed by placing vacancies in either one or both of the boundaries in the supercell. The changes were in a satisfactory range (see later). In addition, we repeated some calculations by inserting an extra stoichiometric layer of atoms in the region between the two boundaries. The vacancy formation energy changed only by 0.2 eV. As will be seen when the results are described, these convergence tests are adequate for the conclusions drawn in this paper.

Figure 1 makes clear that the grain boundary is made of simple repeating structural units. Each unit is a dislocation core that contains a pair of like-ion columns in the center. In “Sr-core” boundaries, the pair of columns contains

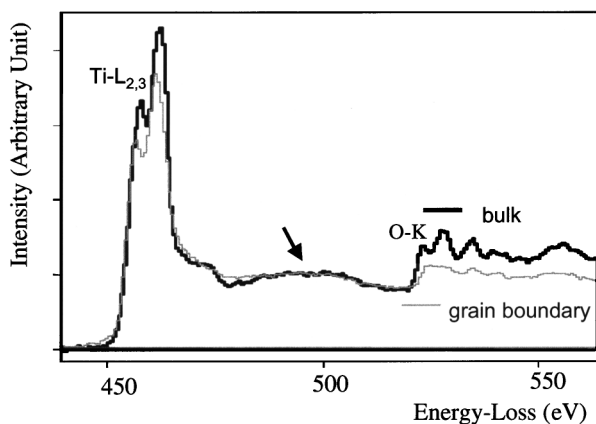


FIG. 2. Energy-loss spectra obtained from the bulk and from an individual dislocation core in an  $8^\circ$  [001] tilt  $\text{SrTiO}_3$  grain boundary. The Ti-L edge continuum shown by the arrow is used for normalization.

only Sr atoms, whereas in “Ti-core” boundaries, the pair of columns contains alternating Ti and O atoms. It was noted in Refs. [11–13] that, if the pair of columns is fully occupied as bulk columns, the boundary is nonstoichiometric. If, however, every other site is occupied, the boundary is stoichiometric. This half-occupation has been described as “reconstruction” [12,13]. Since  $Z$ -contrast intensity in the core of a boundary cannot be normalized relative to that of bulk columns because of local strains, the images are consistent with either possibility. The rationale for preferring stoichiometric boundaries was to avoid like-ion repulsion [12,13].

Evidence for nonstoichiometry comes from EELS. Figure 2 shows the Ti  $L_{2,3}$  and O  $K$  EELS spectra taken in the bulk and at individual dislocation cores of a low-angle  $\text{SrTiO}_3$  grain boundary. Because of nonuniformities in the thickness of the sample, normalization of the two spectra is not automatic. In the figure, we normalized the spectra to the Ti  $L_{2,3}$ -edge continuum, deducing that the intensity of the O  $K$  spectrum from the boundary is significantly lower than from the bulk region. Alternatively, we could normalize the spectra to the O  $K$ -edge continuum, in which case the intensity of the Ti  $L_{2,3}$  spectrum from the boundary would be higher than from the bulk region. The net conclusion is the same, namely, that the ratio of Ti to O concentration in the boundary is higher than the bulk.

In order to explore the relative stability of stoichiometric and nonstoichiometric structures, we performed total-energy calculations using a  $53^\circ$  symmetric  $\{210\}$  [001] tilt grain boundary for which supercells can be constructed from either Sr or Ti units as shown in Fig. 3 (the  $53^\circ$  boundary has the shortest possible period; the  $36^\circ$  boundary used for  $Z$ -contrast images requires larger supercells; the structural units have the same central feature of a pair of columns as shown in Fig. 1). We found distinctly different results for the Sr- and Ti-core boundaries.

Stoichiometric Sr-core boundaries (i.e., two half-full Sr columns) are stable with an excess energy of 21.9 eV/nm<sup>2</sup>. The alternative of having a single, fully occupied Sr column instead of two half-occupied columns was found to have a higher energy (by 0.8 eV/nm<sup>2</sup>). This is consistent with the  $Z$ -contrast images, but further calculations are needed to explore whether nonstoichiometry (e.g., missing O atoms that are not detectable by  $Z$ -contrast imaging) is energetically favored as suggested by EELS. Such calculations will be described later.

In the case of stoichiometric Ti-core boundaries (two half-full Ti-O columns), the excess energy is much larger (33.2 eV/nm<sup>2</sup>) and the alternative of having a single fully occupied Ti-O column has a lower energy. Such a structure is, of course, inconsistent with the  $Z$ -contrast images, leading us to an unambiguous conclusion that the Ti-core boundary must be nonstoichiometric.

In order to explore nonstoichiometry in a Sr-type boundary, we performed calculations of formation energies of O vacancies in various columns surrounding the pair of Sr

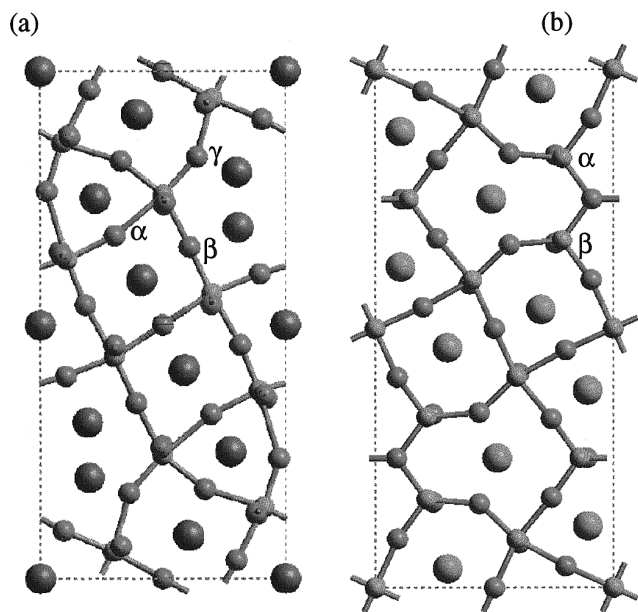


FIG. 3. The relaxed supercell with two  $53^\circ$  symmetric  $\{210\}$   $[001]$  tilt grain boundaries constructed from (a) Sr cores, (b) Ti cores. Sr atoms are shown large.

columns (labeled  $\alpha$ ,  $\beta$ , and  $\gamma$  in Fig. 3) and compared the values with the formation energy of isolated vacancies in the bulk crystal. We found in all cases that vacancies in the boundary are energetically preferred, with the segregation energy varying from 1.3 to 3.5 eV per vacancy. In our supercell, there are only two O atoms per column limiting us to either complete or 50% removal of O atoms. The segregation energies are  $\sim 1$  eV larger for 50% removal. Furthermore, the segregation energy is larger if we remove 50% of two columns instead of 100% of one column. All these results suggest that partial removal of O atoms is energetically preferred, but the optimal O deficiency cannot be established at present. Finally, as an additional test, we compared results when O atoms are removed from only one of the boundaries in the cell versus when O atoms are removed from both boundaries. Segregation energies are larger by  $\sim 1$  eV, which is a measure of the uncertainty in the calculations, but also confirms the conclusion that O vacancies segregate in the boundary.

For the Ti-core boundary, we first considered O deficiency. Recall that, for a stoichiometric Ti-core boundary, we found that a single Ti-O column is energetically preferred over two half-occupied Ti-O columns. When we introduced O vacancies, we found that a single Ti-O column remains energetically preferred. We conclude that O deficiency alone does not produce structures in agreement with the Z-contrast images. Turning to excess Ti, we started with the stoichiometric structure (half-occupied Ti and O sites in the core) and added Ti atoms to fill all available Ti sites. There are two options: (i) all O atoms in one column and (ii) 50% of the O atoms in each column. We used Ti metal for the Ti chemical potential [26] and found an energy reduction in both cases: 1.7 eV/nm<sup>2</sup> for all O atoms in one column, but 3.6 eV/nm<sup>2</sup> for O atoms distributed

between the two columns. Thus, distributing the O atoms in both columns is energetically favored over having them in a single column. The conclusion is, therefore, unambiguous: Ti-core boundaries are nonstoichiometric with excess Ti atoms. With this Ti excess, we now find a negligible segregation energy for O vacancies of 0.3 eV per vacancy. This conclusion is consistent with the Z-contrast images, the EELS spectra, and also with earlier observations [27,28].

We carried out calculations to explore the electronic structure of both stoichiometric and nonstoichiometric grain boundaries in order to determine connections to the “double Schottky barrier” model. We found that the stoichiometric boundaries have a band gap that is essentially the same as in the perfect bulk crystal with the valence bands full, the conduction bands empty, and no energy levels within the gap. In the case of nonstoichiometry with a larger Ti:O ratio, we find the following: an “impurity-band” feature develops at the conduction band edge, which shifts to lower energies. The effect is more pronounced as nonstoichiometry is increased. In all cases, the Fermi energy is within the conduction bands, reflecting the fact that we have excess cation electrons for which there are no corresponding O atoms to provide the necessary valence levels. We calculated the spatial distribution of the electrons in the conduction bands. A typical plot is shown in Fig. 4. It is clear that the excess electrons are localized over the excess Ti atoms, maintaining local charge neutrality. The calculation assumes a pure material. Clearly, in *p*-type material [29], the excess electrons annihilate holes so that the Fermi level remains

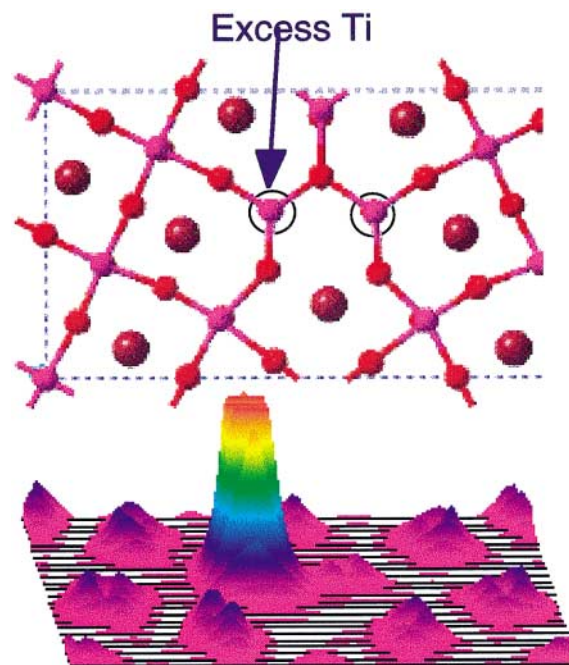


FIG. 4 (color). A half unit cell with excess Ti at a Ti-core grain boundary, and corresponding charge density in the conduction bands from the excess electrons [30]. Two circles show two Ti columns in the core.

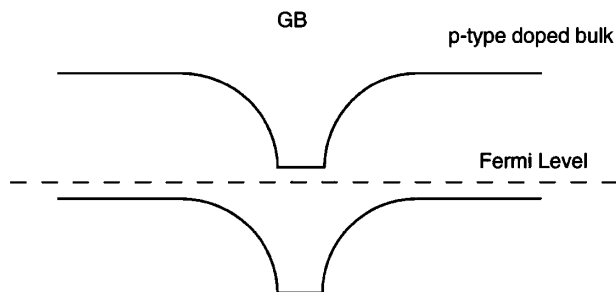


FIG. 5. Nonstoichiometry at the grain boundary sets up a  $p$ - $n$ - $p$  band structure in acceptor-doped bulk.

at the bottom of the energy gap and the grain boundary is charged. In turn, the positively charged boundaries will set up a space-charge region on both sides, bending the bands as shown in Fig. 5. The net result is better described as a  $p$ - $n$ - $p$  double junction than a double Schottky barrier. The grain boundary is really not metallic.

In conclusion, we have used a combination of  $Z$ -contrast imaging, EELS spectra, and first-principles theory to show that grain boundary dislocation cores in  $\text{SrTiO}_3$  are intrinsically nonstoichiometric with a Ti:O ratio that is larger than the bulk value. It is worth noting that each of the three approaches played a distinct and important role. First,  $Z$ -contrast imaging established unambiguously the overall geometric structure of the boundaries, which provides an excellent starting point for theory. Because a  $Z$ -contrast image is not sensitive to O, however, it could not establish if the boundaries are stoichiometric or not. EELS, on the other hand, provided unambiguous evidence for nonstoichiometry. Theory checked which of many possible atomic arrangements are energetically favored and, in conjunction with the  $Z$ -contrast images, ruled out stoichiometric Ti-core boundaries. It further established that O deficiency alone yields a stable structure that is not in agreement with the images; excess Ti alone yields a stable structure that is in agreement with all data. The net conclusion from combining all three techniques is that Ti-core boundaries have excess Ti while Sr-core boundaries have O deficiency. Both effects give excess electrons at the boundary plane which gives rise to the electrical properties.

This research was sponsored by the Division of Materials Sciences, U.S. Department of Energy, under Contract No. DE-AC05-00OR22725 managed by UT-Battelle, LLC, by NSF under Grants No. DMR-9803021, and No. DMR-9803768, and by an appointment to the ORNL postdoctoral research program administered jointly by ORNL and ORISE. Computation time was partially supported by the National Science Foundation under DMR990002N and DMR000004N, and utilized the SGI Origin 2000 at the National Center for Supercomputing Applications, University of Illinois at Urbana-Champaign.

[1] K. D. Johnson and V. P. Dravid, *Appl. Phys. Lett.* **74**, 621 (1990).

- [2] T. Wolfram, *Phys. Rev. Lett.* **29**, 1383 (1972).  
 [3] V. E. Henrich, *Rep. Prog. Phys.* **48**, 1481 (1985).  
 [4] H. Hilgenkamp and J. Mannhart, *Appl. Phys. A, Mater. Sci. Process.* **64**, 553 (1997); H. Hilgenkamp and J. Mannhart, *Appl. Phys. Lett.* **73**, 265 (1998).  
 [5] J. Padilla, W. Zhong, and D. Vanderbilt, *Phys. Rev. B* **53**, R5969 (1996).  
 [6] R. C. Buchanan, T. R. Armstrong, and R. D. Roseman, *Ferroelectrics* **135**, 343 (1992).  
 [7] W. E. Taylor, N. H. Odell, and H. Y. Fan, *Phys. Rev.* **88**, 867–875 (1952).  
 [8] M. Vollman and R. Waser, *J. Am. Ceram. Soc.* **77**, 235–243 (1994).  
 [9] K. L. Kliewer and J. S. Koehler, *Phys. Rev.* **140**, A1226–A1240 (1965).  
 [10] J. A. S. Ikeda and Y.-M. Chiang, *J. Am. Ceram. Soc.* **76**, 2437–2446 (1993).  
 [11] M. M. McGibbon, N. D. Browning, M. F. Chisholm, A. J. McGibbon, S. J. Pennycook, V. Ravikumar, and V. P. Dravid, *Science* **266**, 102 (1994).  
 [12] N. D. Browning, S. J. Pennycook, M. F. Chisholm, M. M. McGibbon, and A. J. McGibbon, *Interface Sci.* **2**, 397–423 (1995).  
 [13] M. M. McGibbon, N. D. Browning, A. J. McGibbon, and S. J. Pennycook, *Philos. Mag. A* **73**, 625 (1996).  
 [14] S. D. Mo, W. Y. Ching, M. F. Chisholm, and G. Duscher, *Phys. Rev. B* **60**, 2416 (1999).  
 [15] I. Dawson, P. D. Bristowe, M.-H. Lee, M. C. Payne, M. D. Segall, and J. A. White, *Phys. Rev. B* **54**, 13727–13733 (1996).  
 [16] S. J. Pennycook and P. D. Nellist, in *Impact of Electron Scanning Probe Microscopy on Materials Research* (Kluwer, Dordrecht, 1999).  
 [17] N. D. Browning, M. F. Chisholm, and S. J. Pennycook, *Nature (London)* **366**, 143 (1993).  
 [18] P. E. Batson, *Nature (London)* **366**, 727 (1993).  
 [19] G. Duscher, N. D. Browning, and S. J. Pennycook, *Phys. Status Solidi A* **166**, 327 (1998).  
 [20] P. Hohenberg and W. Kohn, *Phys. Rev.* **136**, B864 (1964); W. Kohn and L. J. Sham, *Phys. Rev.* **140**, A1133 (1954).  
 [21] D. M. Ceperley and B. J. Alder, *Phys. Rev. Lett.* **45**, 566 (1980).  
 [22] D. Vanderbilt, *Phys. Rev. B* **41**, 7892 (1990).  
 [23] H. J. Monkhorst and J. D. Pack, *Phys. Rev. B* **13**, 5188 (1976).  
 [24] M. C. Payne, M. P. Teter, D. C. Allan, T. A. Arias, and J. D. Joannopoulos, *Rev. Mod. Phys.* **63**, 1045 (1992).  
 [25] S. Kimura, J. Yamauchi, and M. Tsukula, *Phys. Rev. B* **51**, 11049 (1995).  
 [26] C. G. Vandewalle, D. B. Laks, G. F. Neumark, and S. T. Pantelides, *Phys. Rev. B* **47**, 9425 (1993).  
 [27] Y.-M. Chiang and T. Takagi, *J. Am. Ceram. Soc.* **73**, 3278 (1990).  
 [28] R. F. Klie and N. D. Browning, *Appl. Phys. Lett.* **77**, 3737 (2000).  
 [29] D. M. Smyth, *Prog. Solid State Chem.* **15**, 145 (1984).  
 [30] Charge density calculated with WIEN97 (Blaha, Schwarz, and Luitz), a full-potential linearized augmented plane wave package for calculating crystal properties (Technical University, Wien, Austria, 1999); P. Blaha, K. Schwarz, P. Serantin, and S. B. Trickey, *Comput. Phys. Commun.* **59**, 399 (1990).